ISSN: 2834-4928

Research Article

Journal of Electrical Electronics Engineering

Integrated Scheduling Framework for Microgrid Operation Incorporating Conservation Voltage Reduction and Stochastic Demand Response under Short-Term Planning Horizons

Mehdi Nikravan[1], Ghasem Derakhshan[1], Mehdi Hakimi[1] and Bahman Abedi[2*]

[1]*Department of Electrical Engineering, Damavand Branch, Islamic Azad University, Tehran, Iran*

[2]*Department of Electrical Engineering, National University of Skills (NUS), Tehran, Iran*

[*]Corresponding Author
Bahman Abedi, Department of Electrical Engineering, National University of Skills (NUS), Tehran, Iran.
Email Address: abedi.ba@yahoo.com

Submitted: 2025, Mar 17; **Accepted:** 2025, Apr 14; **Published:** 2025, Apr 23

Citation: Nikravan, M., Derakhshan, G., Hakimi, M., Abedi, B. (2025). Integrated Scheduling Framework for Microgrid Operation Incorporating Conservation Voltage Reduction and Stochastic Demand Response under Short-Term Planning Horizons. *J Electrical Electron Eng, 4*(2), 01-17.

Abstract

The strategic planning and operational management of microgrids have become imperative focal points in the evolving landscape of contemporary power systems, predominantly instigated by the pervasive deployment of distributed generation (DG) technologies and the progressive institutionalization of advanced demand response programs (DRPs). The integration of renewable DG resources, inherently characterized by stochastic variability and temporal intermittency, introduces profound layers of uncertainty into the microgrid's day-ahead scheduling and operational paradigm. In response to these challenges, this study delineates a comprehensive stochastic optimization framework for day-ahead microgrid operational planning, wherein the synergistic incorporation of DRPs and Conservation Voltage Reduction (CVR) is pursued to enhance economic optimality and operational robustness. The proposed model concurrently assimilates time-of-use (TOU) pricing schemes and incentive-based demand response modalities. Specifically, TOU programs are employed as load modulation instruments to counteract the volatility of renewable generation, whereas incentive-driven strategies are leveraged to alleviate the inherent commitment uncertainty associated with distributed renewable resources by promoting flexible end-user participation. Moreover, CVR is systematically integrated with voltage-dependent load modeling techniques to facilitate the attenuation of peak demand and improve energy efficiency. The uncertainty associated with renewable energy outputs is rigorously addressed through the Information Gap Decision Theory (IGDT), thereby enabling the formulation of resilient and risk-averse operational strategies under conditions of profound epistemic uncertainty. The resultant non-linear optimization problem is computationally resolved through the deployment of a Genetic Algorithm (GA) applied to a standardized microgrid test system. The obtained simulation outcomes substantiate the proposed framework's capacity to achieve operational cost minimization while concurrently augmenting system reliability and adaptability in the presence of significant uncertainty.

Keywords: Demand Response, Renewable Energy Uncertainty, Conservation Voltage Reduction, Information Gap Decision Theory, Microgrid Optimization

1. Introduction

Conservation Voltage Reduction (CVR) is a critical strategy employed in power distribution systems to maintain voltage levels within regulatory limits, as defined by utility standards. Voltage regulation (VR) can be implemented through various methods depending on system conditions and operational demands. Among these, CVR adjusts the voltage within the permissible range—typically by lowering it—to achieve energy efficiency and economic benefits. CVR has attracted considerable attention due to its potential to reduce operational costs, enhance energy savings, and improve system reliability. By fine-tuning the voltage profile of distribution networks, CVR helps manage load demand and improve overall network efficiency [1,2].

Extensive studies have demonstrated the efficacy of CVR in minimizing peak loads, reducing energy losses, conserving electricity, lowering operational expenditures, and enhancing power system security. For example, presents a comprehensive review of CVR applications and its potential to facilitate energy-efficient and cost-effective operations [3]. In both the advantages and challenges of

CVR are examined, particularly in the context of cost savings and energy conservation [4]. Study optimally applies CVR for microgrid planning, focusing on the sizing and siting of distributed generation (DG) and capacitors to maximize branch efficiency [5]. Similarly, evaluates the energy-saving effects of CVR and voltage optimization in Ireland's distribution network [6]. Research in investigates the use of CVR to reduce energy consumption and manage peak demand, especially under conditions of limited energy availability [7]. Additionally, explores how CVR can enhance system stability, security, and reliability [8].

The integration of voltage regulation with other optimization problems has further advanced multi-objective planning in distribution networks [9]. For instance, proposes a novel framework for simultaneous load scheduling and voltage regulation. Study examines coordinated load-sharing and voltage regulation strategies within microgrids, while addresses the optimal planning of energy storage systems by incorporating CVR effects to minimize both investment and operational costs [10,11]. Other works, such as and, focus on CVR's application in load modeling using machine learning (MSVR) and the use of voltage-current droop characteristics for power consumption reduction, respectively [12,13].

Demand Response Programs (DRPs) are equally crucial for distribution system operators, offering benefits such as reduced operational costs, improved system flexibility, and increased economic returns [14,15]. By shifting or curtailing load during specific periods, DRPs can influence voltage profiles and overall system performance. Prior studies have investigated the interactions between DRPs and voltage regulation, while explores emergency DRPs for real-time voltage control in automated distribution systems [16-18]. Given that DRPs can directly affect voltage levels, it is imperative to examine the combined impact of incentive-based DRPs microgrid performance. The existing literature emphasizes the importance of co-optimizing DRPs and VR to achieve enhanced flexibility and economic performance in modern energy systems [19].

In an integrated DR strategy for microgrids is proposed, enabling autonomous energy bids based on real-time electricity pricing to avoid market conflicts [20]. A market-clearing mechanism with priority-based trading is also introduced to ensure incentive compatibility. Furthermore, investigates the technical, economic, and market implications of CVR in distribution networks. As global electricity demand continues to rise, optimizing voltage levels and energy management becomes increasingly important [21]. Study introduces a novel voltage and VAR management (VVM) model that integrates advanced technologies such as energy storage systems (ESSs), time-of-use DRPs (TOU-DRPs), and photovoltaic (PV) inverters, alongside conventional devices like on-load tap changers (OLTCs) and switchable capacitor banks (SCBs) [22]. In a stochastic bi-level model is developed for coordinated electricity-heat scheduling and storage in microgrids, integrating DRPs and ESSs to maximize social welfare [23]. The focus of these studies lies in the evaluation of incentive-based DRPs under uncertainty [24,25].

1.1 Key Innovations of this Study:

This study introduces a novel approach to managing uncertainty in wind generation through dynamic DR contracts [26,27]. If, for instance, wind generation is forecasted at 12 MW and the actual output deviates by ±1 MW, DR contracts are designed to accommodate this 1 MW range. As the average forecast increases, the corresponding standard deviation also scales linearly, enabling proportional DR adjustments. For example, a forecast of 18 MW with a ±2 MW deviation leads to DR commitments covering that range.

Unlike previous studies that used fixed uncertainty bounds and static DR agreements, this work dynamically adjusts DR contracts based on real-time uncertainty predictions. By considering the statistical relationship between forecasted averages and variability, the approach minimizes over-commitment (which inflates costs) and under-commitment (which leads to load shedding and penalty payments). Two key innovations are emphasized:

Load participation in DRPs is governed by dynamically applied incentive mechanisms rather than fixed incentives.

The uncertainty in renewable generation is modeled using the temporal relationship between forecasted averages and standard deviation, allowing for optimized DRP deployment that enhances reliability and reduces operating costs.

1.2 Paper Organization

The remainder of this paper is structured as follows:
Section II presents the problem formulation, including objective functions and system constraints.
Section III details the proposed CVR strategy and the employed optimization algorithm.
Section IV discusses the simulation setup and analysis.
Section V presents the results and discussion.
Finally, Section VI concludes the paper and outlines future work.

2. Problem Modeling and Notations

2.1 Indices, Functions, Variables, and Parameters

Indices	
i	Generators
t	Time
nWT	The number of wind turbines
	Functions
f_i^{WT}	The function of converting wind speed to wind turbine generation
f_i^{PV}	The function of converting the radiation value into photovoltaic generation
Variables	
revenue	Revenue
Reliability	Reliability
$income$	Income
$cost$	Cost
$P_{i,t}$	The generation rate of unit i at time t
$Cost_{gen}$	Generation cost
$Cost_{res}$	Spining reserve cost
$Cost_{rel}$	Reliability cost
$U_{i,t}$	Binary variable of starting unit i at time t
$K_{i,t}$	Binary variable of unit i being turned on at time t
$\Delta P_{s,t}$	Change in available power due to event s at time t
$\Delta R_{s,t}$	Change of available reservation due to event s at time t
R_t	Total reservation at time t
$p_{s,t}$	The probability of event s at time t
$b_{s,t}$	Binary variable of load shedding due to event s at time t
$C(t)$	The energy in the battery at time t
$EENS$	The expected amount of energy not supplied
$LOLP$	The possibility of load shedding
$R_{i,t}$	The amount of reservation of unit i at time t
P_t^E	Battery generation or consumption power
Parameters	
$C_{i,t}$	Baseline generation cost per MW
$q_{i,t}$	Spining reservation cost per MW
SC_i	The cost of setting up unit i
$VOLL$	Lost load value
$LOLP_t^{max}$	The maximum probability of acceptable load shedding at time t

P_t^D	Load value at time t
P_i^{max}	Generation capacity of unit i
P_i^{min}	The minimum generation by unit i
RUR_i	The maximum slope of the increase in the generation by unit i
τ	Time steps
$v_{i,t}^{actual}$	The actual wind speed value at time t
$v_{i,t}^{fcst}$	The forecasted wind speed value at time t
$g_{i,t}^{trun}$, $g_{i,t}^{fcst}$	Max battery charge/discharge rate
P_{max}^E	The maximum battery capacity
d_T	Battery charge efficiency
C_E , C_S	Initial and final battery charge levels
C_{max} , C_{min}	Battery capacity limits
du_T	Duration of each outages

2.2 Objective Function and Constraints: Baseline Model

This model is a multi-objective optimization problem targeting short-term power system operations, emphasizing both economic efficiency and reliability. The two primary objectives are maximizing revenue and ensuring system reliability.

2.3 Objective Functions

$$\max(\text{revenue},). \tag{1}$$

$$\text{revenue} = income - cost \tag{2}$$

$$income = \sum_{t=1}^{T}\sum_{i=1}^{I} MP(t).P_{i,t} \tag{3}$$

$$cost = Cost_{gen} + Cost_{res} + Cost_{rel} \tag{4}$$

$$Cost_{gen} = \sum_{t=1}^{T}\sum_{i=1}^{I}\left[C_{i,t}\left(P_{i,t}, U_{i,t}\right) + SC_i.K_{i,t}\right] \tag{5}$$

$$Cost_{res} = \sum_{t=1}^{T}\sum_{i=1}^{I} q_{i,t}R_{i,t} \tag{6}$$

$$Cost_{rel} = EENS \times VOLL \tag{7}$$

The first objective seeks to maximize revenue, calculated as power sale income minus operational costs (generation, reserve, and reliability). The second objective targets system reliability, represented by the Loss of Load Probability (LOLP):

$$\text{Reliability}= LOLP \tag{8}$$

To ensure system reliability, the probability of load shedding must not exceed a predefined threshold:

$$LOLP_t \leq LOLP_t^{max} \tag{9}$$

Key Constraints

Power Balance Constraint

$$\sum_{i=1}^{I} P_{i,t} = P_t^D \qquad \forall t \tag{10}$$

Spinning Reserve Capability Constraint:

$$R_{i,t} \leq \min(U_{i,t}(RUR_i\tau), P_i^{max}U_{i,t} - P_{i,t}) \tag{11}$$

2.4 Battery Energy Storage System (ESS) Modeling

The battery can charge and discharge subject to the following technical constraints:
Charge/Discharge Limit:

$$|P_t^E| \leq P_{max}^E \tag{12}$$

$Energy\ Evolution$:

$$C(t+1) = C(t) - d_T P_t^{Edc}\eta^E + d_T P_t^{Ec}/\eta^E \tag{13}$$

Initial and Final Charge Levels:

$$C(0) = C_S\,, C(T) = C_E \tag{14}$$

Initial and Final Charge Levels:

$$C_{min} \leq C(t) \leq C_{max} \tag{15}$$

Where P_t^{Edc} and P_t^{Ec} represent the discharge and charge power of the battery, respectively. P_{max}^E is the maximum allowable charging or discharging power, and η^E denotes the efficiency of the charging/discharging process. The parameter, d_T is the duration of each time step (in hours), and $C(t)$ is the energy stored in the battery at time t. The battery must maintain energy levels between specified bounds, with C_S and C_E being the initial and final energy levels, and C_{min} and C_{max} representing the minimum and maximum battery capacity, respectively.

Similar to the battery system, the upstream power grid is modeled as both a power source and sink, depending on system needs. Its interaction with the microgrid is constrained by the capacity of the communication transformer connecting the two. The cost of importing electricity from, or exporting to, the upstream grid is based on the prevailing wholesale market price.

2.5 Demand Response Program Modeling

As previously discussed, two types of Demand Response Programs (DRPs) are considered in this study: incentive-based programs and price-based programs such as Time-of-Use (TOU), Real-Time Pricing (RTP), and Critical Peak Pricing (CPP). The main objective of DRP modeling is to ensure that the total electricity cost for consumers is reduced after program participation, without compromising their comfort. The model also captures the tendency of loads to participate in DRPs.

2.5.1 Incentive-Based Program

For incentive-based DR, the goal is to minimize the electricity cost by reducing or shedding a portion of the load. The optimization objective is formulated as follows [6]:

$$F_{i/c} = f(x) = min \sum_{t=1}^{T}(PD^t \times x^t \times EP^t) \tag{16}$$

Subject to:

$$0.7 < x^t < 1$$

Where EP^t is the price of electricity in each time interval t, PD^t is the electricity demand of shedabble loads at time t, and x^t is the decision variable indicating the load reduction level, allowing up to 30% of load to be shed.

Consumers participating in this program are incentivized with a rebate equal to the electricity price at the time of shedding.

2.5.2 Price-Based Programs (TOU, RTP, CPP)

In price-based DRPs, the cost of power consumption is influenced by the program type. The total cost for TOU and CPP participants is expressed as follows [2]:

$$F_{t\&r} = min: (1 - \gamma_1 - \gamma_2 - \gamma_3) \sum_{t=1}^{T} EP^t * d_0(t) + \sum_{t=1}^{T} \rho(t) * d_e(t) \quad (17)$$

$$d_e(t) = (\gamma_1 + \gamma_2 + \gamma_3) * d_0(t)(1 + \sum_{k=1}^{T} E(t.k) * \frac{\rho(k) - EP^t}{EP^t}) \quad (18)$$

The percentage of participation in each of these programs is a variable, that is, some shiftable loads are contributed in the TOU program, some in the real-time pricing (RTP) program, and some in the CPP program. The sum will be 1. Since the TOU and CPP programs follow the same equation, Equation (17) is written for them. The only difference between these two programs in equation (18) is the design of pricing $\rho(k)$ .In the TOU program, a three-level tariff is considered for off-peak, mid-peak, and on-peak hours, and in the RTP program, this tariff is changed hourly.

The participation percentages, γ_1, γ_2, and γ_3 must sum to one, and their optimal values are determined during the optimization process.

2.5.3 Critical Peak Pricing (CPP) via Cobb-Douglas Model

To model consumer response under CPP, the Cobb-Douglas production function is applied to account for the effects of both price and ambient temperature on electricity consumption [7]:

$$Q(t) = A\, P^{ep}(t) W^{ew}(t) \quad (19)$$

$$A = \gamma_3 * d_0(t) \quad 20)$$

Where $Q(t)$ is the consumption of loads participating in the critical peak pricing program after the implementation of the program, A is the constant coefficient of the load value which is a percentage of the initial shiftable load, P is the price of electricity, W is the ambient temperature, *ep* is the dependence of charge on price, and *ew* is the dependence of charge on temperature. As the price increases, the consumption will decrease, and as the temperature increases, the consumption will increase. Taking the logarithm from the sides of Equation (19) and assuming that we represent the logarithm of each variable with its small symbol, we have:

$$q(t) = A + ep * p(t) + ew * w(t) + U(t) \quad (21)$$

The parameters, *ep* and *ew* are estimated using the least squares method to minimize the total error:

$$\phi(a.ep.ew) = \sum_{i=1}^{T} U(t)^2 \sum_{i=1}^{T} [q(t) - (a + ep * p(t) + ew * w(t))]^2 \quad (22)$$

These parameters are solved using simultaneous equations, based on historical consumption, pricing, and temperature data.

2.6 Modeling the Load Response Uncertainty Using the IGDT Method

In the **Information-Gap Decision Theory (IGDT)** method, a set of possible uncertainties is defined, and the objective function, which depends on parameters subject to uncertainty, is optimized to be flexible in the face of these input uncertainties.

This section considers the participation rate in the **Demand Response Program (DRP)** as a non-deterministic parameter and evaluates how its effects on the problem can be controlled. Therefore, parameters **γ_1 to γ_3** are treated as non-deterministic according to the model.

The problem formulation is represented by equations (23) to (26), incorporating a risk-aversion strategy. The risk-averse strategy is selected because the problem is not risk-tolerant. The objective is to make the system as resistant as possible to the uncertainty in load participation. This is critical because any deviation in the participation rate, compared to the predicted value under a risk-taking strategy, may lead to an imbalance between generation and consumption. Such an imbalance is unacceptable for the grid operator.

$$\Re_C = \underset{X\,.\,\alpha}{max}\ \alpha \tag{23}$$

$$f < f_b(X.\gamma) \times (1+\beta).\gamma \in \Gamma \tag{24}$$

$$f_b(X.\gamma) = \underset{X}{max}\ f.\gamma = \bar{\gamma} \tag{25}$$

$$\gamma = \bar{\gamma} \times (1-\alpha) \tag{26}$$

Where X represents the decision variable, including the spot prices and the value of the proposed load shedding. α is the radius of uncertainty, and β is the percentage of deviation from the objective function in the risk-aversion strategy.

2.7 Load Management through CVR

One of the innovative approaches to reducing energy consumption and peak load without directly interfering with the consumption patterns of end-users is Conservation Voltage Reduction (CVR). This method facilitates load reduction by controlling the voltage of the consumption buses to a minimum level, ensuring that the system's security is not compromised. This is crucial, as a significant portion of the load is inherently dependent on the voltage range.

Different types of loads exhibit varying responses to voltage reductions. For instance, the power consumed by cooling loads decreases as their voltage is reduced. However, these systems must operate for a longer duration to reach the desired temperature, as they are operating with less power. Therefore, their overall energy consumption remains unaffected. In contrast, the energy consumption and power of other load categories may decrease when the voltage is reduced. Additionally, some loads, particularly those operating at constant power, experience minimal change in response to voltage fluctuations. Consequently, the response rate of a given grid to CVR is contingent upon the specific model and characteristics of its loads. According to existing studies, the application of CVR typically results in a reduction of energy consumption ranging from 0.5% to 4%.

To assess the impact of CVR on the optimal utilization of a microgrid, grid load distribution equations must be examined alongside objective functions and constraints. The modeling of this problem incorporates a radial grid structure, voltage-dependent loads, on-load tap-changer (OLTC) transformers, and shunt capacitors.

In the radial structure, the number of branches equals the number of nodes minus one. The system's initial bus, denoted as bus number 0, serves as the connection point between the distribution grid and the transmission system, with a constant voltage range. The load distribution equations for each branch are as follows:

$$P_{ij} - \sum_{k\in N_j} P_{jk} = \frac{r_{ij}\left(P_{ij}^2 + Q_{ij}^2\right)}{V_i^2} - p_j \tag{27}$$

$$Q_{ij} - \sum_{k\in N_j} Q_{jk} = \frac{x_{ij}\left(P_{ij}^2 + Q_{ij}^2\right)}{V_i^2} - q_j \tag{28}$$

$$V_i^2 - V_j^2 = 2\left(r_{ij}P_{ij} + x_{ij}Q_{ij}\right) - \frac{(r_{ij}^2 + x_{ij}^2)(P_{ij}^2 + Q_{ij}^2)}{V_i^2} \tag{29}$$

$$p_j = p_j^g - p_j^d\ , q_j = q_j^g - q_j^d + q_j^c \tag{30}$$

Where i represents the bus number, and p_j, q_j, and v_j denote the injected active power, injected reactive power, and voltage at bus j, respectively. The subscript *ij*, refers to the line between buses i and j, with r_{ij}, x_{ij}, P_{ij}, and Q_{ij} representing the resistance, reactance, active power, and reactive power of line *ij*,, respectively. The superscript d denotes the load component. The load is modeled using the ZIP model, and the relationship between load and voltage is given by the following equations:

$$p_j^d(V_j) = P_{0,j}^d \left[P_{Z,j} \left(\frac{V_j}{V_{0,j}} \right)^2 + P_{I,j} \left(\frac{V_j}{V_{0,j}} \right) + P_{P,j} \right] \tag{31}$$

$$q_j^d(V_j) = Q_{0,j}^d \left[Q_{Z,j} \left(\frac{V_j}{V_{0,j}} \right)^2 + Q_{I,j} \left(\frac{V_j}{V_{0,j}} \right) + Q_{P,j} \right] \tag{32}$$

Where the subscript 0 indicates the load value at nominal voltage, and the subscripts Z, I, and P refer to constant impedance, constant current, and constant power.

The model of transformers with OLTC is represented as a device between buses *ij*. with the following load distribution equations:

$$P_{ij} - \sum_{k \in N_j} P_{jk} = \frac{r_{ij}\left(P_{ij}^2 + Q_{ij}^2\right)}{V_i^2 / a_{ij}^2} - p_j \tag{33}$$

$$Q_{ij} - \sum_{k \in N_j} Q_{jk} = \frac{r_{ij}\left(P_{ij}^2 + Q_{ij}^2\right)}{V_i^2 / a_{ij}^2} - q_j \tag{34}$$

$$\frac{V_i^2}{a_{ij}^2} - V_j^2 = 2\left(r_{ij}P_{ij} + x_{ij}Q_{ij}\right) - \frac{\left(r_{ij}^2 + x_{ij}^2\right)\left(P_{ij}^2 + Q_{ij}^2\right)}{V_i^2 / a_{ij}^2} \tag{35}$$

$$\underline{a}_{ij} \le a_{ij} \le \overline{a}_{ij} \tag{36}$$

Where a_{ij} represents the tap ratio, constrained between its minimum and maximum values. Additionally, the shunt capacitor is modeled as a parallel susceptance at the corresponding bus, with its injected reactive power depending on the voltage level. The susceptance value can be varied between 0 and its maximum allowable value:

$$q_i^c(V_i) = B_i^c V_i^2 \tag{37}$$

$$0 \le B_i^c \le \overline{B_i^c} \tag{38}$$

According to IEEE Std. 1547-2018, distributed generation (DG) resources are classified into two categories based on their reactive power capacity and voltage regulation ability: resources with limited voltage regulation (suitable for systems with low penetration coefficients) and those with greater voltage regulation capacity (typically found in systems with higher penetration coefficients). This study focuses on resources with significant voltage control capabilities.

The active and reactive power outputs of these resources are constrained by their capability curve and are mathematically represented by the following equations:

$$a1_i^r s_i^r \le p_i^g \le a2_i^r s_i^r \tag{39}$$

$$b1_i^r p_i^g \le q_i^g \le b2_i^r p_i^g \tag{40}$$

$$c1_i^r s_i^r \le q_i^g \le c2_i^r s_i^r \tag{41}$$

Four operational modes for voltage-power control of the source are considered: constant power factor, voltage-reactive power, active power-reactive power, and constant reactive power. The relationship between active and reactive power in these four modes is described by the following equations:

$$q_i^g(p_i^g) = \tan(\emptyset_i)p_i^g \quad (42)$$

$$q_i^g(V_i) = -m_q(V_i - V_{i,ref}) \quad (43)$$

$$q_i^g(p_i^g) = -b_q(p_i^g - P_{rated}) \quad (44)$$

3. Simulation Results

The scenarios for non-deterministic parameters, including wind, load, and solar generation, are based on the data presented in [8]. The grid topology, which will be provided in the final section of the numerical studies, will facilitate the analysis of the **Conservation Voltage Reduction (CVR)** results.

In this study, a microgrid is examined numerically. The characteristics of load behavior and energy pricing in the upstream grid are outlined in [2]. Subscribers consume power at a fixed rate of 15 cents per kWh, and the upstream grid rate is utilized for power exchange between the microgrid and the main grid.

Elasticity matrices for **Time-of-Use (TOU)** and **Real-Time Pricing (RTP)** programs are derived from [24]. Figures 1 through 3 illustrate the pricing structures for the three programs.

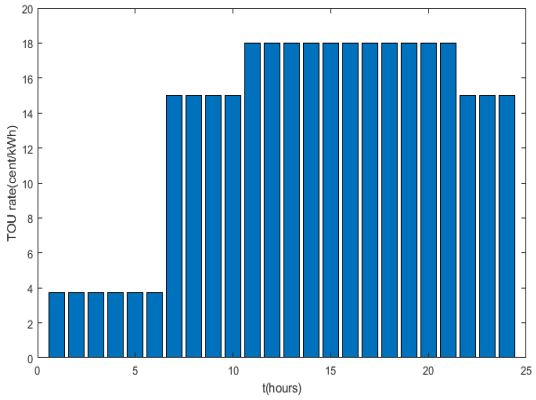

Figure 1: TOU Program

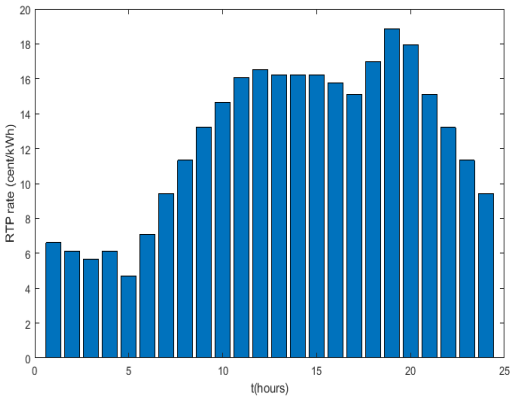

Figure 2: RTP Program

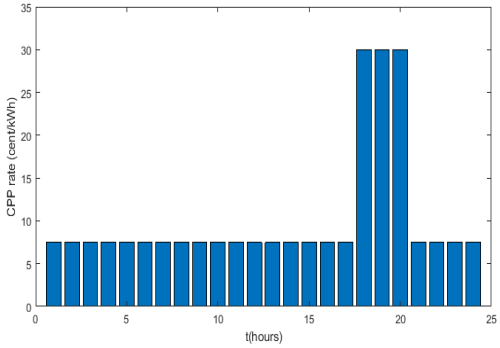

Figure 3: CPP Program

3.1 Simulation Without Considering Demand Response (DR)

The simulations are conducted under several case studies. The results are first presented in Section 3.1 as a single-objective optimization problem, excluding the load shedding penalty. Subsequently, in Section 3.1.3, the results are shown as single-objective optimization with the inclusion of the load shedding penalty. Finally, the problem is solved as a bi-objective optimization problem that incorporates the load shedding penalty.

3.1.1 Numerical Results without Load Shedding Penalty

In this section, the hourly load supply cost, generation rate, and reservation value for the Genetic Algorithm (GA) are presented. The total cost for this scenario is 15,778.67 cents. The hourly Loss of Load Probability (LOLP) values are depicted in Figure 4.

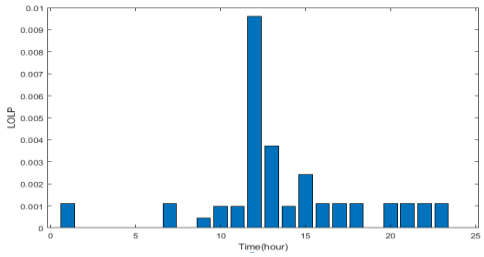

Figure 4: Hourly LOLP Without Load Shedding Penalty

The expected value of lost energy over 24 hours, as calculated by the GA, is 0.187 kWh.

3.1.2 Simulation Results with Load Shedding Penalty

For this scenario, the total cost of providing load is 16,703.97 cents. The LOLP values, as shown in Figure 5, are reflective of the inclusion of the load shedding penalty.

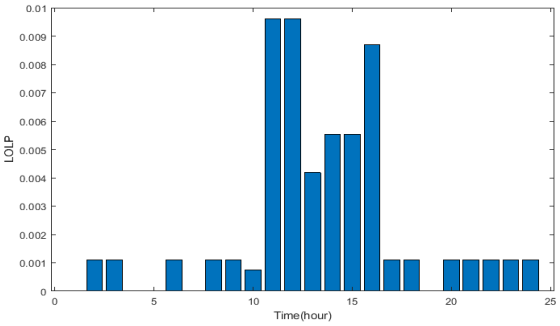

Figure 5: Hourly LOLP With Load Shedding Penalty

The expected value of lost energy is calculated as 0.357 kWh. It is important to note that the load interruption penalty and reservation cost represent two conflicting objectives in the optimization process.

3.1.3 Simulation Results with Bi-Objective Load Shedding Penalty

In this case, the total cost of supplying the load is 16,902.19 cents. The LOLP values are illustrated in Figure 6.

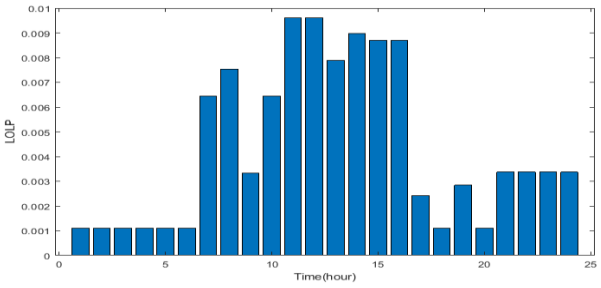

Figure 6: Hourly LOLP With Bi-Objective Load Shedding Penalty

Additionally, Figure 7 presents the hourly cost under this multi-target scenario.

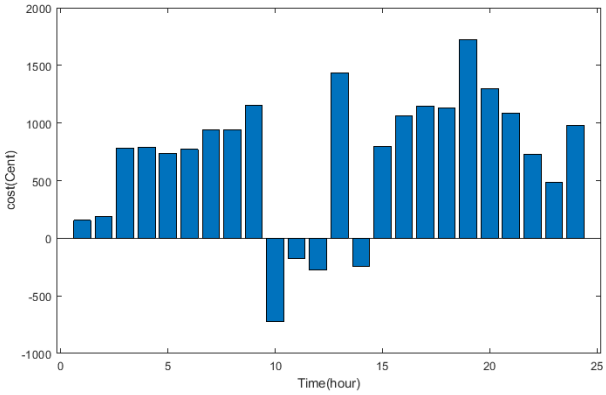

Figure 7: Hourly Cost With Bi-Objective Load Shedding Penalty

The expected value of lost energy in this case is 0.263 kWh, and the total cost is 16,902 cents. For a comparative analysis, the results are summarized in Table 2, which compares the solutions obtained using three different solution methods.

Algorithm	Without penalty-single objective		With penalty-single objective		Bi-objective	
	Cost	EENS	Cost	EENS	Cost	EENS
GA	15778	0.607	16702	0.478	16902	0.263

Table 2: Comparison of Solutions

According to the table, the cost shows an increasing trend as load shedding penalty is incorporated. In the first case study, where there is no load shedding penalty, the reservation is allocated solely to meet the LOLP constraint, resulting in a lower cost. In the second study, the inclusion of the load shedding penalty leads to a higher cost, but the reliability (measured by EENS) improves as a result. This improvement in reliability is attributable to the load shedding penalty embedded in the objective function. Lastly, the third study, which utilizes a bi-objective approach, incurs a higher cost compared to the second study. This is due to the simultaneous optimization of both the reliability and cost objectives, as opposed to focusing solely on cost in the second study

3.2 Simulation Considering Demand Response (DR)

The ambient temperature, which models the participation rate of subscribers in the Critical Peak Pricing (CPP) program, is illustrated in Figure 8. The parameters *ep* and *ew*, used in the modeling of CPP, are set to -0.83 and 1.2085, respectively.

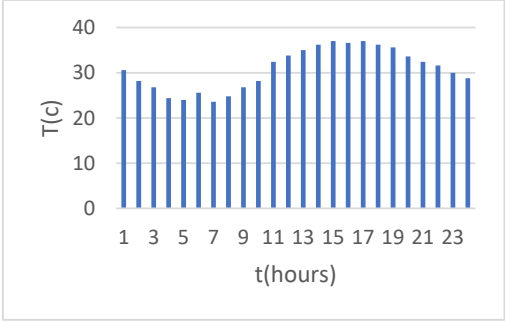

Figure 8: Ambient Temperature Over 24 Hours

Figures 9 and 10 present the results of the Time-of-Use (TOU) programs under two scenarios, with 5% and 10% participation rates applied to the load curve. The updated load for shedding in these two scenarios is shown for the different components of the program. The critical peak values of ew and ep are 1.2085 and -0.83, respectively, corresponding to the pricing program. This study is conducted under two distinct scenarios, 5% and 10% participation in the TOU programs, to provide a clearer comparison.

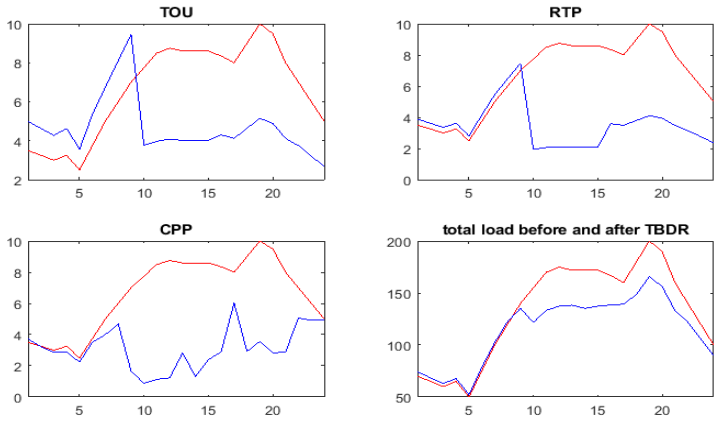

Figure 9: Updated Load for 5% Participation in the TOU Programs

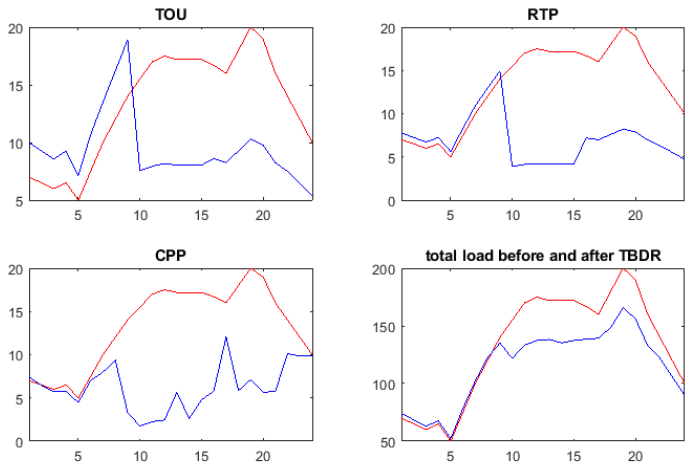

Figure 10: Updated load for 10% Participation in the TOU Programs

3.2.1 Simulation Considering Interruptible Load Program and 5% Participation in the TOU Program

In the previous section, the cost paid by the loads for supplying electrical energy was constant and amounted to 45,793.5 cents. However, in this section, loads participate voluntarily in demand response programs. The costs associated with loads participating in the Time-of-Use (TOU) programs before and after participation are compared in Table 3. These programs are voluntary and should be designed such that the amount received from the load is greater than the total payment made to the resources. This ensures the feasibility of their implementation, while also generating additional revenue for the loads when they participate.

Program	Cost Before Participation (cents)	Cost After Participation (cents)
TOU	1686.864	1520.229
RTP	1258.030	1022.785
CPP	1118.823	768.739

Table 3: Comparison of the Cost of the Loads Participating in TOU Programs Before And After Implementation (5% Participation)

In this way, the loads are incentivized to participate in the TOU program. The total cost function value in this scenario is 16,423.78 cents.

3.2.2 Simulation Considering Interruptible Load Program and 10% Participation in the TOU Program

The cost of responsive demands before and after the implementation of the program is shown in Table 4. For all three programs, the cost after participation exceeds the cost before participation, indicating the correct design of the Demand Response Program (DRP).

Program	Cost before participation (cent)	Cost after participation (cent)
TOU	3373.728	3040.457
RTP	2516.061	2045.571
CPP	2237.647	1537.479

Table 4: Comparison of the Cost of the Loads Participating in TOU Programs Before and After Implementation (10% Participaation)

The value of interruptible load is determined during the optimization process due to its inherent variability. This value will be provided later in the study. The total cost function value in this mode is 12,679.66 cents.

3.3 Incorporating the Uncertainty of Responsive Demand Participation

In this section, the uncertainty associated with the participation of responsive demands in demand response programs is modeled using the Info-Gap Decision Theory (IGDT) framework introduced in Chapter 3. In previous sections, fixed participation scenarios were considered: 0% and 10% for interruptible loads, and 5% and 10% for responsive loads. These discrete scenarios were used to demonstrate the effect of participation rate on the objective function outcomes. To enhance this analysis, three scenarios are examined for responsive demands, as summarized in Table 5, to illustrate the impact of varying participation levels.

Objective function	TOU program	Incentive-based program
16902	0	0
16423	5	10
12060	10	10

Table 5: Cost Objective Function Values for Various Demand Response Participation Scenarios

As seen in the table, initial changes in participation have a minor impact on the objective function, while later increases yield significant cost reductions. This non-linear and non-intuitive response underscores the need to consider the uncertainty of load participation within DRPs. Since such uncertainty often negatively affects the objective function, a **risk-averse strategy** is adopted via the IGDT model. The goal is to ensure the robustness of the objective function in the presence of deviations from the expected participation levels.

To this end, a risk-averse solution is derived under the assumption of a 10% participation rate with a 10% deviation. The results, compared with the base case (objective function value of 12,060 cents), reveal that such a deviation could lead to a **40% increase in cost**, indicating a significant impact and validating the use of robust modeling.

A sensitivity analysis is then performed on:

- The **uncertainty radius** of responsive demand participation (α),
- The **permissible increase** in the objective function (β), and
- Different **Loss of Load Probability (LOLP)** values.

The uncertainty radius is divided equally between incentive-based and time-based demands. The sensitivity analysis assumes that β varies from 5**% to 15% in 2.5% increments**, and LOLP ranges from 1**% to 5% in 1% increments**. The resulting uncertainty radii are plotted in **Figure 11**.

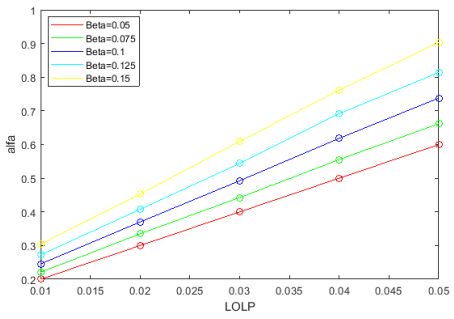

Figure 11: Uncertainty Radius vs. LOLP for Different βs Values

(Description: As LOLP decreases, the permissible uncertainty radius also decreases. A larger β allows for a higher uncertainty radius at the same LOLP.)

Next, **Figure 12** illustrates how the uncertainty radius changes with β for different LOLP levels. When the x-axis is normalized to the percentage deviation of the objective function from its baseline, **Figure 13** is obtained.

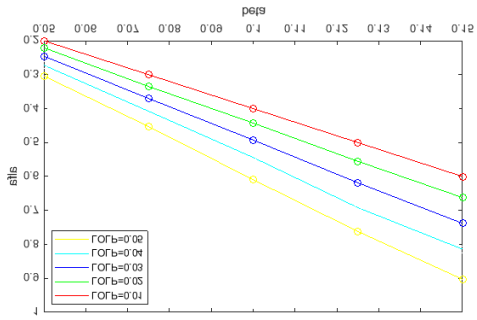

Figure 12: Uncertainty Radius vs. Objective Function Deviation (β) for Different LOLP Levels

(Observation: The uncertainty radius decreases as LOLP constraints become stricter. Sensitivity to β is low for small values.)

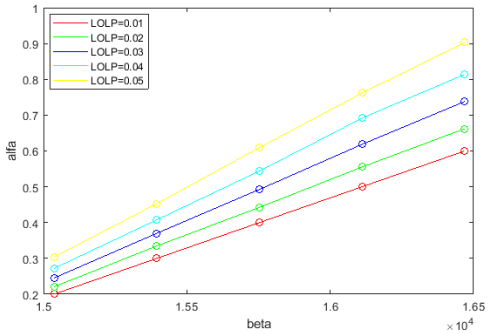

Figure 13: Operating Cost Impact vs. Uncertainty Radius for Various LOLPs

(Interpretation: Guaranteeing a lower LOLP while maintaining a larger uncertainty radius increases system operating costs.)

To evaluate the value of using a risk-averse strategy, the following two cases are analyzed:
Case 1 (Reactive Strategy):

Assuming 10% participation was forecasted, but in reality, only 5% was achieved (i.e., 5% deviation). Applying corrective action using spinning reserves results in a **total system cost of 13,982 cents**, which is **1,922 cents** higher than the base case (12,060 cents).
Case 2 (Risk-Averse Strategy):

The forecast assumes a 10% participation with a 5% risk buffer. If full 10% participation is realized (i.e., better than expected), the total system cost drops to **12,611 cents**, which is **410 cents** lower than the conservative cost estimate of **13,021 cents** from the risk-averse solution.
This comparison demonstrates that:

The **potential cost overrun** in the first case (1,922 cents) is significantly higher than the cost **overestimation** in the second case (410 cents).

Thus, applying a **risk-averse strategy reduces exposure** to adverse outcomes due to participation uncertainty.

Moreover, in Case 1, the actual operating cost (13,982 cents) surpasses the estimate from the risk-averse strategy (13,021 cents), underscoring the importance of accounting for uncertainty in DRPs.

3.4 Integration of Grid Topology and Conservation Voltage Reduction (CVR)

In this section, the underlying distribution network, including its topology and the technical specifications of its branches, is incorporated into the analysis. The grid under study corresponds to the standard IEEE 13-bus test system. The hourly load profile remains consistent with the scenarios discussed in preceding sections.

To accurately reflect the voltage sensitivity of the loads, the ZIP model is employed in the load flow analysis. Consequently, the final energy consumption is marginally reduced relative to the nominal value, as a portion of the load demand is inherently dependent on the voltage level at each bus.

The impact of implementing CVR on the hourly load demand, after incorporating demand response (DR) programs, is illustrated in Figure 14. The figure presents a comparative analysis of the load profile before and after the application of CVR, highlighting the overall reduction in demand achieved through voltage optimization.

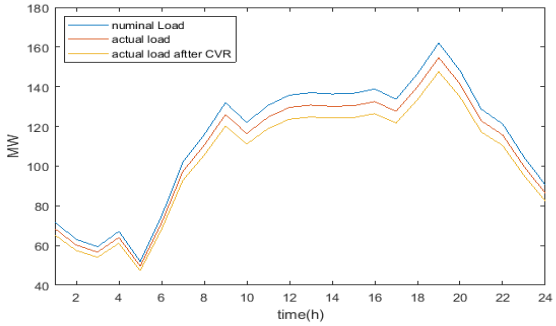

Figure 14: Comparison of hourly load before and after applying CVR (post-DR implementation)

4. Discussions

The key insights obtained from the numerical simulations and analysis are as follows:

• **Impact of Load Shedding Penalty on System Cost**:

Incorporating the load shedding penalty into the objective function results in a higher total cost of supplying both the load and spinning reserve. This is expected, as the addition of a new cost component increases the overall objective value. To compensate, the system may reduce reserve levels, thereby increasing the load shedding index. Therefore, for the load shedding penalty to be effective in improving system reliability, its assigned value must be sufficiently high to disincentivize reserve reduction.

• **Blackout Risk in High-Impact, Low-Probability Events**:

The relatively low LOLP value at the cost-reliability equilibrium point indicates that blackouts are primarily caused by rare but high-impact events. These events, while infrequent, significantly influence the expected energy not supplied (EENS), even though their effect on the LOLP index is minimal.

• **Scenario-Based Reserve Allocation**:

Incremental reserves are allocated to mitigate power shortages resulting from variability in load, wind, and solar generation. However, the generation scheduling is based on the most probable scenario. In some cases, surplus generation may occur, which can be curtailed using wind or solar resources.

• **Forecast Accuracy and Real-Time Feasibility**:

Since the prediction error decreases as the forecasting time horizon shortens—and because the proposed optimization algorithm operates within a few minutes—non-deterministic parameters can be forecast with reasonable accuracy using this approach.

• **Cost-Reliability Trade-Off Assessment via EENS:**

The trade-off between system cost and reliability should be analyzed using the EENS index, as it directly represents a cost-equivalent metric. This allows for straightforward integration into the objective function when improving reliability by increasing reserves.

• **Benefits of Demand Response Participation:**

Demand response programs (DRPs) significantly improve both the cost of load supply and system reliability. Although announced load curtailments introduce additional costs, these are negligible compared to the reductions in generation and reserve costs, as well as in unplanned outage penalties, thus validating the value of DRPs.

• Risk-Averse Strategy via IGDT:
As the uncertainty in responsive demand participation increases, modeling this uncertainty through IGDT and applying a risk-averse strategy protects the operator from a steep rise in costs. This strategy ensures a more stable operational environment.

• Cost Risk Without Considering Participation Uncertainty:
If the uncertainty in load participation is neglected, the actual operating cost may exceed that obtained under the risk-averse strategy, especially when the predicted levels of participation are not realized.

• Effectiveness of CVR in Cooling Loads:
The addition of CVR in the grid context shows limited impact on energy consumption by cooling loads. During peak hours, these loads require a fixed energy input due to thermal demand. Although power is reduced under CVR, the compressor run-time increases, leading to minimal net energy reduction.

• DR Impact Despite Minimal Energy Savings from CVR:
Even though CVR does not significantly reduce energy consumption for cooling loads, it does lower power demand, resulting in approximately 3% improvement in DR program performance.

5. Conclusion

To extend the scope of this research and guide future studies, the following directions are recommended:
• Integrated Renewable and Storage Systems:
To ensure dispatchable and flexible power from renewable energy sources, it is advisable to consider their integration with storage systems in future studies.

• Reliability Evaluation Using Deterministic Criteria:
This study employed a probabilistic reliability approach, evaluating events up to the second order. Future work should include comparisons with deterministic reliability criteria such as N−1 or N−2, to enhance the robustness of the reliability framework.

• Scenario Correlation Modeling:
It is recommended to incorporate the correlation between uncertain parameters (load, wind, and solar radiation) in scenario generation. Randomly combining uncorrelated scenarios can misrepresent actual operating conditions, leading to inaccurate solutions.

• DRP Pricing Based on Extreme Scenarios:
DR program pricing should be designed in accordance with deviations in the worst-case scenarios relative to average conditions. This will provide stronger economic incentives for loads to shift or reduce consumption when it is most beneficial to the system.

• Adoption of IGDT for Broader Uncertainty Modeling:
Given the effectiveness of IGDT in addressing uncertainties, it is suggested to expand its application to model uncertainties in wind, load, and grid stress, replacing conventional scenario-based approaches for more robust decision-making.

• CVR in Extended Distribution Networks:
In this study, CVR was implemented in a small-scale distribution network where voltage drop was not a critical issue. Future investigations should apply CVR to extended radial networks, where voltage regulation poses a greater challenge, potentially revealing additional operational complexities.

References

1. Das, S., & Basu, M. (2020). Day-ahead optimal bidding strategy of microgrid with demand response program considering uncertainties and outages of renewable energy resources. *Energy, 190*, 116441.
2. Thirugnanam, K., El Moursi, M. S., Khadkikar, V., Zeineldin, H. H., & Al Hosani, M. (2020). Energy management of grid interconnected multi-microgrids based on P2P energy exchange: A data driven approach. *IEEE Transactions on Power Systems, 36*(2), 1546-1562.
3. Kermani, M., Shirdare, E., Parise, G., Bongiorno, M., & Martirano, L. (2022). A comprehensive technoeconomic solution for demand control in ports: Energy storage systems integration. *IEEE Transactions on Industry Applications, 58*(2), 1592-1601.
4. Nizami, M. S. H., Hossain, M. J., & Mahmud, K. (2020). A coordinated electric vehicle management system for grid-support services in residential networks. *IEEE Systems Journal, 15*(2), 2066-2077.
5. Ramos, F. O., Pinheiro, A. L., Lima, R. N., Neto, M. M., Junior, W. A., & Bezerra, L. G. (2021, September). A real case analysis of a battery energy storage system for energy time shift, demand management, and reactive control. In *2021 IEEE PES Innovative Smart Grid Technologies Conference-6. Latin America (ISGT Latin America)* (pp. 1-5). IEEE.

6. Helmi, H., Abedinzadeh, T., Beiza, J., and Daghigh, A. (2023). "Day-ahead operation planning of microgrids considering conservation voltage reduction (CVR) and uncertainty-based demand response." SSRN Electronic Journal. Jan.
7. Muttaqi, K. M., & Sutanto, D. (2021). Adaptive and predictive energy management strategy for real-time optimal power dispatch from VPPs integrated with renewable energy and energy storage. *IEEE Transactions on Industry Applications, 57*(3), 1958-1972.
8. Tran, V. T., Islam, M. R., Muttaqi, K. M., & Sutanto, D. (2019). An efficient energy management approach for a solar-powered EV battery charging facility to support distribution grids. *IEEE Transactions on Industry Applications, 55*(6), 6517-6526.
9. Pertl, M., Carducci, F., Tabone, M., Marinelli, M., Kiliccote, S., & Kara, E. C. (2018). An equivalent time-variant storage model to harness EV flexibility: Forecast and aggregation. *IEEE transactions on industrial informatics, 15*(4), 1899-1910.
10. Mokaramian, E., Shayeghi, H., Sedaghati, F., Safari, A., & Alhelou, H. H. (2022). An optimal energy hub management integrated EVs and RES based on three-stage model considering various uncertainties. *IEEE Access, 10*, 17349-17365.
11. Rehman, A. U., Wadud, Z., Elavarasan, R. M., Hafeez, G., Khan, I., Shafiq, Z., & Alhelou, H. H. (2021). An optimal power usage scheduling in smart grid integrated with renewable energy sources for energy management. *IEEE access, 9,* 84619-84638.
12. Avula, R. R., Chin, J. X., Oechtering, T. J., Hug, G., & Månsson, D. (2021). Design framework for privacy-aware demand-side management with realistic energy storage model. *IEEE Transactions on Smart Grid, 12*(4), 3503-3513.
13. Ali, S., Kazmi, S. A. A., Malik, M. M., Bhatti, A. H. U., Haseeb, M., Kazmi, S. M. R., & Shin, D. R. (2021). Energy management in high RER multi-microgrid system via energy trading and storage optimization. *IEEE Access, 10,* 6541-6554.
14. Rafique, S., Hossain, M. J., Nizami, M. S. H., Irshad, U. B., & Mukhopadhyay, S. C. (2021). Energy management systems for residential buildings with electric vehicles and distributed energy resources. *IEEE Access, 9,* 46997-47007.
15. Antoniadou-Plytaria, K., Steen, D., Carlson, O., & Ghazvini, M. A. F. (2020). Market-based energy management model of a building microgrid considering battery degradation. *IEEE transactions on smart grid, 12*(2), 1794-1804.
16. Zhou, S., Chen, Z., Huang, D., & Lin, T. (2020). Model prediction and rule-based energy management strategy for a plug-in hybrid electric vehicle with hybrid energy storage system. *IEEE Transactions on Power Electronics, 36*(5), 5926-5940.
17. Chen, H., Xiong, R., Lin, C., & Shen, W. (2020). Model predictive control based real-time energy management for hybrid energy storage system. *CSEE Journal of Power and Energy Systems, 7*(4), 862-874.
18. Şengör, İ., Erdinç, O., Yener, B., Taşcıkaraoğlu, A., & Catalão, J. P. (2018). Optimal energy management of EV parking lots under peak load reduction-based DR programs considering uncertainty. *IEEE Transactions on Sustainable Energy, 10*(3), 1034-1043.
19. Karimi, H., Gharehpetian, G. B., Ahmadiahangar, R., & Rosin, A. (2023). Optimal energy management of grid-connected multi-microgrid systems considering demand-side flexibility: A two-stage multi-objective approach. *Electric Power Systems Research, 214*, 108902.
20. Zhang, Z., Huang, Y., Chen, Z., & Lee, W. J. (2022). Integrated demand response for microgrids with incentive compatible bidding mechanism. *IEEE Transactions on Industry Applications, 59*(1), 118-127.
21. Fakour, A., Jodeiri-Seyedian, S. S., Jalali, M., Zare, K., Tohidi, S., Zadeh, S. G., & Shafie-Khah, M. (2023). Investigating impacts of CVR and demand response operations on a bi-level market-clearing with a dynamic nodal pricing. *IEEE Access, 11,* 19148-19161.
22. Gholami, K., Azizivahed, A., Arefi, A., & Li, L. (2023). Risk-averse Volt-VAr management scheme to coordinate distributed energy resources with demand response program. *International Journal of Electrical Power & Energy Systems, 146*, 108761.
23. Yang, Z., Tian, H., Min, H., Yang, F., Hu, W., Su, L., & SaeidNahaei, S. (2023). Optimal microgrid programming based on an energy storage system, price-based demand response, and distributed renewable energy resources. *Utilities Policy, 80*, 101482.
24. Vardakas, J. S., Zorba, N., & Verikoukis, C. V. (2014). A survey on demand response programs in smart grids: Pricing methods and optimization algorithms. *IEEE Communications Surveys & Tutorials, 17*(1), 152-178.
25. Khanbabaee, M. M., & Abedi, B. (2023). A probabilistic load flow comparison in distribution systems by performing optimal capacitors/DERs sizing and placement, simultaneously.
26. Abedi, B., Ghadimi, A. A., Abolmasoumi, A. H., Miveh, M. R., & Jurado, F. (2021). An improved TPM-based distribution network state estimation considering loads/DERs correlations. *Electrical Engineering, 103*(3), 1541-1553.
27. Daemi, T., Pourfarzin, S. and Akbari, H. (2024). "Day-ahead operation scheduling of microgrids considering conservation voltage reduction and uncertainty-based demand response programs." *Int. J. Smart Electr. Eng*., vol. 13, no. 1, pp. 33–52, Winter.